

Analytical control of small molecules by intense laser pulses in an algebraic model

Hairan Feng,¹ Yan Liu,^{1,2} Yujun Zheng,^{1,*} Shiliang Ding,¹ and Weiyi Ren²

¹*School of Physics and Microelectronics, Shandong University, Jinan 250100, China*

²*School of Physics and Electronic Information, China West Normal University, Nanchong 637002, China*

(Received 26 March 2007; revised manuscript received 24 April 2007; published 21 June 2007)

In this paper, we study the laser-pulse control of vibrational excitation for small molecules by employing an algebraic model. The analytical expression for the vibrational transition probability is obtained by using an algebraic approach. Selective vibrational excitation of diatomic and linear triatomic molecules are achieved. The influence of laser pulse frequencies and shapes on the control are studied.

DOI: [10.1103/PhysRevA.75.063417](https://doi.org/10.1103/PhysRevA.75.063417)

PACS number(s): 32.80.Rm, 33.80.Rv, 03.65.Fd

I. INTRODUCTION

The quantum control of problem by laser is an active subject both in theoretical and experimental areas [1–5]. Studies of the quantum control are motivated by a fundamental interest in quantum properties of light, and the possible applications in physics, chemistry, quantum computation, cryptology, etc. Comprehensive reviews can be found in Refs. [6–9]. One receiving considerable attention in this field is selective vibrational excitation and dissociation, which is important for controlling the chemical reaction and the quantum states on demand. Various approaches are suggested, for example, the pump-dump laser, optimal control theory, phase control, etc. Much of the work, however, has studied the problem by solving the time-dependent Schrödinger equation (TDSE). The Floquet method has also been employed to study the problem of molecules in intense laser fields. The development of generalized Floquet formalisms allows the reduction of the periodical or a quasiperiodical time-dependent Schrödinger equation into a set of time-independent coupled equations or a Floquet matrix eigenvalue problem. But the Floquet method has usually been used to discuss the atomic problems, and it becomes complicated for the molecules [10–13].

In this work we present an algebraic model on the control of vibrational excitation for small molecules. In the algebraic framework we can obtain the explicit expression of the time-evolution operator directly. The time-evolution operator can be expressed as a product of a finite number of exponential operators if the operators in the Hamiltonian close under commutation. The parameters in the time-evolution operator satisfy a set of differential equations. In past years, the application of time-dependent problems of the dynamical Lie algebraic approach have been advanced. Algebraic methods have been extensively used to study problems in nuclear physics, molecular physics, quantum optics, etc., for example, the problems of vibrational excited states and potential energy surfaces for small polyatomic molecules have been solved successfully [14–19]. This approach was recently used to study the interacting quantum system, the dynamical symmetries and their breaking in nanophysics, the Tavis-Cummings problem and the decoherence in a general

three-level system, the dynamical entanglement of vibrations, etc. [20–25]. In the present work, the control of both diatomic and triatomic molecules are studied in the algebraic framework. We make a comparison with other numerical results and we get a good agreement. The influences of laser pulse frequencies and shapes on control are discussed.

This paper is structured as follows. In Sec. II we derived the time-evolution operator of the system by using the algebraic method for the diatomic and triatomic molecules. The analytical expression of the transition probability is obtained via the time-evolution operator. In Sec. III we discussed the selective vibrational excitation of OH and OD by shaped and chirped laser pulses and the multiphoton excitation problem. For triatomic molecules, we calculated the selective bond excitation of HCN and DCN molecules in the linear chirped laser pulses with different shapes. The problem of intramolecular vibrational redistribution (IVR) is also discussed in this section. The paper ends with some concluding remarks in Sec. IV.

II. THEORETICAL BACKGROUND

A. General considerations

The present work studies the control problem of small molecules (diatomic and triatomic molecules) in the laser field via algebraic approaches. The more ambitious case of including another environment is not pursued at this time. The Hamiltonian of the system can be written as

$$\mathcal{H} = \mathcal{H}_{\text{mol}} + \mathcal{V}, \quad (1)$$

where \mathcal{H}_{mol} is the Hamiltonian of an unperturbed molecule and \mathcal{V} is its interaction with a laser field. As usual, we consider here the interaction between the molecule and the laser field within the electric dipole approximation,

$$\mathcal{V} = -\boldsymbol{\mu} \cdot \boldsymbol{\mathcal{E}}(t), \quad (2)$$

where $\boldsymbol{\mathcal{E}}(t)$ is the external laser field and $\boldsymbol{\mu}$ is the molecular dipole moment.

It is suitable to consider this problem in *the interaction representation*. The Hamiltonian (1) could be split into an \mathcal{H}_0 part and an additional “interaction” \mathcal{H}' , namely, the Hamiltonian (1) can be rewritten as

*yzheng@sdu.edu.cn

$$\mathcal{H} = \mathcal{H}_0 + \mathcal{H}'(t). \quad (3)$$

In the interaction representation, the system Hamiltonian is written as

$$\mathcal{H}_I(t) = e^{i\mathcal{H}_0 t/\hbar} \mathcal{H}'(t) e^{-i\mathcal{H}_0 t/\hbar}, \quad (4)$$

and the time-evolution operator is given by

$$i\hbar \frac{\partial}{\partial t} \mathcal{U}_I(t) = \mathcal{H}_I(t) \mathcal{U}_I(t), \quad (5)$$

with the initial condition $\mathcal{U}_I(t=0)=1$.

Once we know the evolution operator of the system, we can extract all the information of the system from the evolution operator. Here we are specially interested in the transition probability of the system from the initial state $|v_i\rangle$ to the final state $|v_f\rangle$,

$$\mathcal{P}_{v_i, v_f}(t) = |\langle v_f | \mathcal{U}_I(t) | v_i \rangle|^2. \quad (6)$$

The corresponding long-time average probability is defined as

$$\bar{\mathcal{P}}_{v_i, v_f} = \lim_{T \rightarrow \infty} \left\{ \frac{1}{T} \int_0^T \mathcal{P}_{v_i, v_f}(t) dt \right\}. \quad (7)$$

Here we neglect the obvious labels of the various aspects of the laser field in Eqs. (6) and (7). In the following sections we would obtain the obvious expressions of Eqs. (6) and (7) in the theoretical framework.

B. Theoretical framework for diatomic molecules

We consider here the one-dimensional vibrational motion of a diatomic molecule. The $U(2)$ algebra is successfully applied to describe vibrations; the Hamiltonian of a nonrotating Morse oscillator could be written as [26–29]

$$\mathcal{H}_{\text{mol}} = \hbar\omega_0 \left(\hat{A}^\dagger \hat{A} + \frac{\hat{I}_0}{2} \right), \quad (8)$$

where ω_0 is the frequency of the anharmonic oscillator. The creation (\hat{A}^\dagger) and annihilation (\hat{A}) operators obey the commutation relations [26],

$$\begin{aligned} [\hat{A}, \hat{A}^\dagger] &= \hat{I}_0, \\ [\hat{I}_0, \hat{A}] &= -2\chi_0 \hat{A}, \\ [\hat{I}_0, \hat{A}^\dagger] &= 2\chi_0 \hat{A}^\dagger. \end{aligned} \quad (9)$$

It should be noted that \hat{I}_0 is an operator and tends to the identity operator in the harmonic limits, and $\chi_0 \rightarrow 0$ in these limits. The anharmonic correction is given in the order of $\chi_0 = 1/N$.

In our numerical calculation we would replace N by $N+1$. According to Cooper *et al.* [28,29], this modification can lead to quite accurate fits to the vibrational energy levels of diatomic molecules, potential function including the zero-point energy, and achieve the known value of dissociation energy.

The molecular dipole moment $\boldsymbol{\mu}(x)$ could be expanded in a series at the equilibrium, and we keep the first order in our present work, as in Refs. [30–33], i.e.,

$$\boldsymbol{\mu}(x) = \boldsymbol{\mu}x. \quad (10)$$

The interaction between the molecule and the laser field, Eq. (2), can be rewritten as

$$\mathcal{V} = -\frac{d(t)}{2} (\hat{A}^\dagger + \hat{A}), \quad (11)$$

where the time-dependent parameter $d(t)$ is

$$d(t) = \boldsymbol{\mu} \cdot \boldsymbol{\mathcal{E}}(t) \frac{1}{\alpha} \sqrt{\frac{\hbar\omega_0}{D}}. \quad (12)$$

Here we choose $\mathcal{H}_0 = \mathcal{H}_{\text{mol}}$ and $\mathcal{H}' = \mathcal{V}$, the system Hamiltonian, in the interaction representation from Eq. (4), reads

$$\begin{aligned} \mathcal{H}_I(t) &= e^{i\mathcal{H}_0 t/\hbar} \mathcal{V} e^{-i\mathcal{H}_0 t/\hbar} \\ &= e^{i\omega_0 \chi_0 t \hat{A}^\dagger \hat{A}} e^{i\omega_0 t/2} d(\hat{A}^\dagger + \hat{A}) e^{-i\omega_0 t/2} e^{-i\omega_0 \chi_0 t \hat{A}^\dagger \hat{A}} \\ &= d e^{i\omega_0 \chi_0 t} e^{i\omega_0 t/2} \hat{A}^\dagger d e^{i\omega_0 \chi_0 t} e^{-i\omega_0 t/2} \hat{A} \\ &\equiv \gamma_+ \hat{A}^\dagger + \gamma_- \hat{A}. \end{aligned} \quad (13)$$

Here we have taken the operator \hat{I}_0 as an identity approximately in the exponential term since the anharmonic correction is of order χ_0 . It is often of the order of 1% or less for realistic molecules [26].

Since the generators \hat{A}^\dagger , \hat{A} , and \hat{I}_0 form a closed Lie algebra [see Eq. (9)], the evolution operator can be written as [23,34,35]

$$\mathcal{U}_I = e^{-(i\hbar)\mu_0 \hat{I}_0} e^{-(i\hbar)\mu_+ \hat{A}^\dagger} e^{-(i\hbar)\mu_- \hat{A}}, \quad (14)$$

where the coefficients $\mu_r(t)$ ($r=0, +, -$) are known as the Lagrange parameters [34]. The equations of the Lagrange parameters $\mu_r(t)$ are given by

$$\dot{\mu}_0 = -\frac{i}{\hbar} \mu_+ \gamma_- e^{(i\hbar)2\chi_0 \mu_0},$$

$$\dot{\mu}_+ = \gamma_+ e^{-(i\hbar)2\chi_0 \mu_0} - \frac{\chi_0}{\hbar^2} \mu_+^2 \gamma_- e^{(i\hbar)2\chi_0 \mu_0},$$

$$\dot{\mu}_- = \gamma_- e^{(i\hbar)2\chi_0 \mu_0}, \quad (15)$$

with the initial conditions

$$\mu_r(t=0) = 0 \quad (r=0, \pm). \quad (16)$$

The probability from the initial state $|v_i\rangle$ to the final state $|v_f\rangle$, from Eq. (6), is

$$\mathcal{P}_{v_i, v_f}(t) = |\langle v_f | \mathcal{U}_I(t) | v_i \rangle|^2 = |\lambda(t)|^2 \delta_{v_f, v_i - m + n}, \quad (17)$$

where

$$\begin{aligned} \lambda(t) = & \exp\left\{-\frac{i}{\hbar}\mu_0[1-2\chi_0(v_i-m+n)]\right\} \sum_{n=0}^{\infty} \frac{1}{n!} \left(-\frac{i}{\hbar}\mu_+\right)^n \\ & \times \sqrt{\prod_{n'=0}^n [1-\chi_0(v_i-m'+n'-1)](v_i-m'+n')} \\ & \times \sum_{m=0}^{\infty} \frac{1}{m!} \left(-\frac{i}{\hbar}\mu_-\right)^m \\ & \times \sqrt{\prod_{m'=0}^m [1-\chi_0(v_i-m')(v_i-m'+1)]}. \end{aligned} \quad (18)$$

The analytic expression of vibrational transition probability is obtained and we can tackle many concrete examples using this expression.

C. Theoretical framework for triatomic molecules

As a natural extension in this subsection, here we consider the control of the triatomic molecule. The triatomic molecule could be thought of as the two coupled Morse oscillators, i.e., the dynamical symmetry group of a triatomic molecule is

$$U_1(2) \otimes U_2(2). \quad (19)$$

For stretching vibrations in a triatomic molecule, the algebraic Hamiltonian reads [36]

$$\begin{aligned} \mathcal{H}_{\text{mol}} = & \hbar\omega_{01} \left(\hat{A}_1^\dagger \hat{A}_1 + \frac{\hat{I}_{01}}{2} \right) + \hbar\omega_{02} \left(\hat{A}_2^\dagger \hat{A}_2 + \frac{\hat{I}_{02}}{2} \right) \\ & - \lambda(\hat{A}_1^\dagger \hat{A}_2 + \hat{A}_2^\dagger \hat{A}_1), \end{aligned} \quad (20)$$

where the “1” and “2” subscripts denote one of the two bonds of the molecule, respectively, λ is the coupling coefficient, and we include here the kinetic and potential linear couple terms. ω_{01} and ω_{02} are the angular frequencies of bond 1 and bond 2 of the triatomic molecule, respectively.

The interaction between the triatomic molecule and the laser field can be expressed, similar to the diatomic molecule, as

$$\mathcal{V} = d_1(t)(\hat{A}_1^\dagger + \hat{A}_1) + d_2(t)(\hat{A}_2^\dagger + \hat{A}_2), \quad (21)$$

where

$$\begin{aligned} d_1(t) = & -\frac{1}{2\alpha_1} \sqrt{\frac{\hbar\omega_{01}}{D_1}} \boldsymbol{\mu}_1 \cdot \boldsymbol{\mathcal{E}}(t), \\ d_2(t) = & -\frac{1}{2\alpha_2} \sqrt{\frac{\hbar\omega_{02}}{D_2}} \boldsymbol{\mu}_2 \cdot \boldsymbol{\mathcal{E}}(t). \end{aligned} \quad (22)$$

Here the linear dipole moment form is employed for the molecule [37].

In the interaction picture, the Hamiltonian of the system for the triatomic molecule is

$$\begin{aligned} \mathcal{H}_I(t) = & e^{i\mathcal{H}_0 t/\hbar} \mathcal{H}' e^{-i\mathcal{H}_0 t/\hbar} \\ = & d_1(t)(\kappa_{1+} \hat{A}_1^\dagger + \kappa_{1-} \hat{A}_1) + d_2(t)(\kappa_{2+} \hat{A}_2^\dagger + \kappa_{2-} \hat{A}_2) \\ & - \lambda(\kappa_{1+} \kappa_{2-} \hat{A}_2^\dagger \hat{A}_2 + \kappa_{1-} \kappa_{2+} \hat{A}_2^\dagger \hat{A}_1), \end{aligned} \quad (23)$$

where

$$\kappa_{j+} = e^{i\omega_{0j}(x_{0j} + I_{0j})t},$$

$$\kappa_{j-} = e^{i\omega_{0j}(x_{0j} - I_{0j})t} \quad (j=1,2). \quad (24)$$

In the calculation we have chosen

$$\mathcal{H}_0 = \hbar\omega_{01} \left(\hat{A}_1^\dagger \hat{A}_1 + \frac{\hat{I}_{01}}{2} \right) + \hbar\omega_{02} \left(\hat{A}_2^\dagger \hat{A}_2 + \frac{\hat{I}_{02}}{2} \right),$$

$$\mathcal{H}' = -\lambda(\hat{A}_1^\dagger \hat{A}_2 + \hat{A}_2^\dagger \hat{A}_1) + d_1(t)(\hat{A}_1^\dagger + \hat{A}_1) + d_2(t)(\hat{A}_2^\dagger + \hat{A}_2). \quad (25)$$

We partition the Hamiltonian (23), for the simplicity of algebraic structure and calculation, into two parts

$$\mathcal{H}_I(t) = \mathcal{H}_I^{(0)} + \mathcal{H}_I^{(1)}(t), \quad (26)$$

where we let

$$\mathcal{H}_I^{(0)} = d_1(\kappa_{1+} \hat{A}_1^\dagger + \kappa_{1-} \hat{A}_1) + d_2(\kappa_{2+} \hat{A}_2^\dagger + \kappa_{2-} \hat{A}_2) \quad (27)$$

and

$$\mathcal{H}_I^{(1)}(t) = -\lambda(\kappa_{1+} \kappa_{2-} \hat{A}_1^\dagger \hat{A}_2 + \kappa_{1-} \kappa_{2+} \hat{A}_2^\dagger \hat{A}_1). \quad (28)$$

It is easily shown that the operator in Hamiltonian (27) closes under the commutation (9). The time-evolution operator $\mathcal{U}_I^{(0)}$, corresponding to Hamiltonian (27), can be written as [23,34,35]

$$\begin{aligned} \mathcal{U}_I^{(0)} = & e^{-(i\hbar)\mu_{01}\hat{I}_{01}} e^{-(i\hbar)\mu_{1+}\hat{A}_1^\dagger} e^{-(i\hbar)\mu_{1-}\hat{A}_1} e^{-(i\hbar)\mu_{02}\hat{I}_{02}} \\ & \times e^{-(i\hbar)\mu_{2+}\hat{A}_2^\dagger} e^{-(i\hbar)\mu_{2-}\hat{A}_2}. \end{aligned} \quad (29)$$

Following procedures similar to those carried out in the preceding section, the Lagrange parameters are satisfied:

$$\begin{aligned} \dot{\mu}_{01} = & -\frac{i}{\hbar} d_1 \kappa_{1-} \mu_{1+} e^{(i\hbar)2\chi_{01}\mu_{01}}, \\ \dot{\mu}_{1+} = & d_1 \kappa_{1+} e^{-(i\hbar)2\chi_{01}\mu_{01}} - \frac{\chi_0}{\hbar^2} d_1 \kappa_{1-} \mu_{1+}^2 e^{(i\hbar)2\chi_{01}\mu_{01}}, \\ \dot{\mu}_{1-} = & d_1 \kappa_{1-} e^{(i\hbar)2\chi_{01}\mu_{01}}, \\ \dot{\mu}_{02} = & -\frac{i}{\hbar} d_2 \kappa_{2-} \mu_{2+} e^{(i\hbar)2\chi_{02}\mu_{02}}, \\ \dot{\mu}_{2+} = & d_2 \kappa_{2+} e^{-(i\hbar)2\chi_{02}\mu_{02}} - \frac{\chi_{02}}{\hbar^2} d_2 \kappa_{2-} \mu_{2+}^2 e^{(i\hbar)2\chi_{02}\mu_{02}}, \\ \dot{\mu}_{2-} = & d_2 \kappa_{2-} e^{(i\hbar)2\chi_{02}\mu_{02}}. \end{aligned} \quad (30)$$

The initial conditions are $\mu_r(t=0)=0$ ($r=01, 1\pm, 02, 2\pm$).

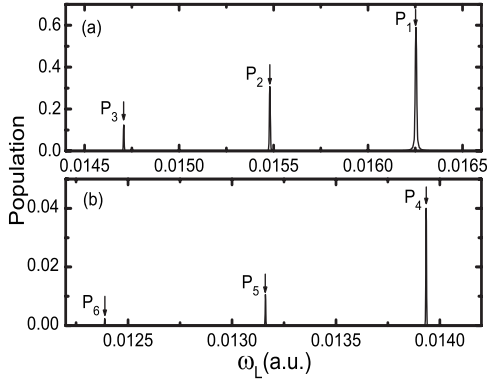


FIG. 1. Long-time average populations of OH as a function of laser frequency. (a) The transitions from the ground state to the first, second, and third excited states. (b) The transitions from the ground state to the fourth, fifth, and sixth excited states. P_i ($i=1, \dots, 6$) denotes the transition $|v=0\rangle \rightarrow |v=i\rangle$.

If $\mathcal{U}_I^{(0)}(t)$ is known, the evolution operator $\mathcal{U}_I(t)$ describing the whole system [corresponding total Hamiltonian (23)] will be given by [38]

$$\mathcal{U}_I(t) = \mathcal{U}_I^{(0)}(t) \cdot \mathcal{U}_I^{(1)}(t), \quad (31)$$

where $\mathcal{U}_I^{(1)}(t)$ satisfies the evolution equation

$$i\hbar \frac{\partial}{\partial t} \mathcal{U}_I^{(1)}(t) = \mathcal{H}_I^{(1)'}(t) \mathcal{U}_I^{(1)}(t), \quad (32)$$

with the initial condition $\mathcal{U}_I^{(1)}(0)=1$. The Hamiltonian $\mathcal{H}_I^{(1)'}(t)$ is given by [38]

$$\mathcal{H}_I^{(1)'}(t) = \mathcal{U}_I^{(0)\dagger}(t) \mathcal{H}_I^{(1)}(t) \mathcal{U}_I^{(0)}(t). \quad (33)$$

The Hamiltonian $\mathcal{H}_I^{(1)'}(t)$ can be then expressed as

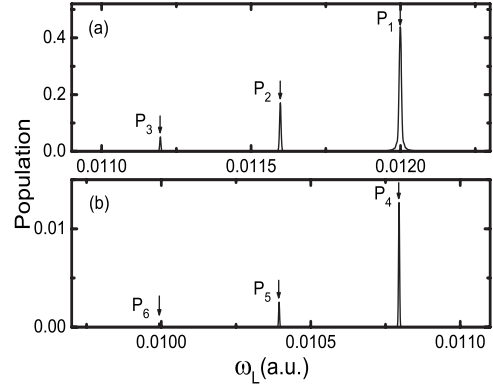


FIG. 2. Long-time average populations of OD as a function of laser frequency. The others are the same as Fig. 1.

$$\begin{aligned} \mathcal{H}_I^{(1)'}(t) &= (\mathcal{U}_I^{(0)})^{-1} \mathcal{H}_I^{(1)}(t) \mathcal{U}_I^{(0)} \\ &= \beta_0 \hat{I}_{01} \hat{I}_{02} + \beta_1 \hat{I}_{02} \hat{A}_1^\dagger + \beta_2 \hat{I}_{02} \hat{A}_1 + \beta_3 \hat{I}_{01} \hat{A}_2^\dagger + \beta_4 \hat{I}_{01} \hat{A}_2 \\ &\quad + \beta_5 \hat{A}_1^\dagger \hat{A}_2 + \beta_6 \hat{A}_1 \hat{A}_2^\dagger + \beta_7 \hat{A}_1^\dagger \hat{A}_2^\dagger + \beta_8 \hat{A}_1 \hat{A}_2, \end{aligned} \quad (34)$$

where

$$\begin{aligned} \beta_0 &= \frac{\eta_1}{\hbar^2} \mu_{1-} \mu_{2+} \left(1 - \frac{\chi_{02}}{\hbar^2} \mu_{2+} \mu_{2-} \right) \\ &\quad + \frac{\eta_2}{\hbar^2} \mu_{1+} \mu_{2-} \left(1 - \frac{\chi_{01}}{\hbar^2} \mu_{1+} \mu_{1-} \right), \end{aligned}$$

$$\beta_1 = -\frac{i}{\hbar} \eta_1 \mu_{2+} \left(1 - \frac{\chi_{02}}{\hbar^2} \mu_{2+} \mu_{2-} \right) + \frac{i}{\hbar^3} \eta_2 \chi_{01} \mu_{1+}^2 \mu_{2-},$$

$$\begin{aligned} \beta_2 &= -\frac{i}{\hbar^3} \eta_1 \chi_{01} \mu_{1-}^2 \mu_{2+} \left(1 - \frac{\chi_{02}}{\hbar^2} \mu_{2+} \mu_{2-} \right) \\ &\quad + \frac{i}{\hbar} \eta_2 \mu_{2-} \left(1 - \frac{\chi_{01}}{\hbar^2} \mu_{1+} \mu_{1-} \right)^2, \end{aligned}$$

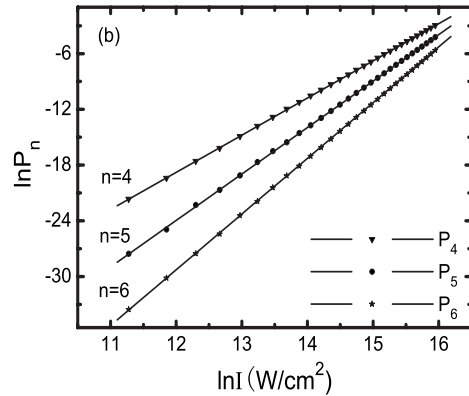
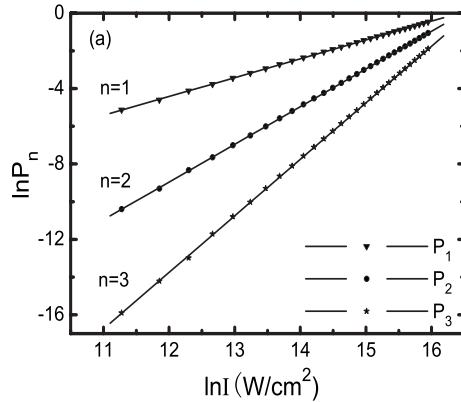


FIG. 3. Log-log plots of the transition populations of OH as a function of laser intensity. n is the slope of the log-log plots. (a) The transitions from the ground state to the first, second, and third excited states. (b) The transitions from the ground state to the fourth, fifth, and sixth excited states. The meaning of P_i is the same as Fig. 1. The data calculated are plotted as dots and the lines are fitted linear lines. It should be noted that the n is kept as the integer since it is the photon numbers.

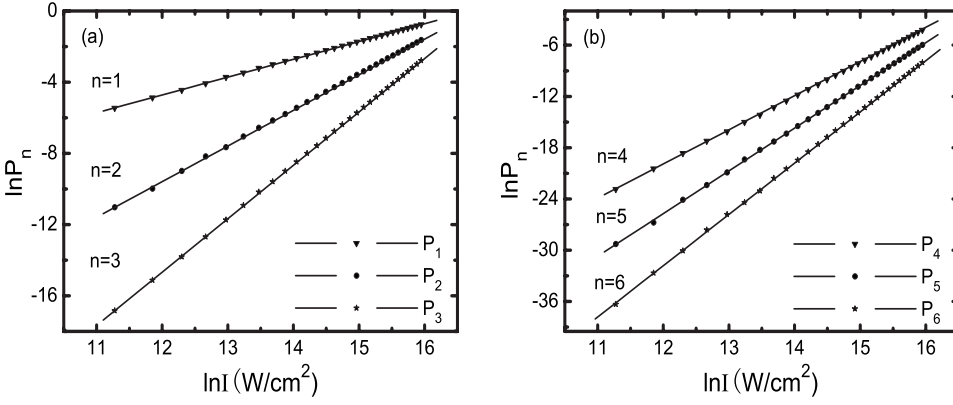


FIG. 4. Log-log plots of the transition populations of OD as a function of laser intensity. The others are the same as Fig. 3.

$$\beta_3 = \frac{i}{\hbar^3} \eta_1 \chi_{02} \mu_{1-} \mu_{2+}^2 - \frac{i}{\hbar} \eta_2 \mu_{1+} \left(1 - \frac{\chi_{01}}{\hbar^2} \mu_{1+} \mu_{1-} \right),$$

$$\beta_4 = \frac{i}{\hbar} \eta_1 \mu_{1-} \left(1 - \frac{\chi_{02}}{\hbar^2} \mu_{2+} \mu_{2-} \right)^2 - \frac{i}{\hbar^3} \eta_2 \chi_{02} \mu_{1+} \mu_{2-}^2 \left(1 - \frac{\chi_{01}}{\hbar^2} \mu_{1+} \mu_{1-} \right),$$

$$\beta_5 = \eta_1 \left(1 - \frac{\chi_{02}}{\hbar^2} \mu_{2+} \mu_{2-} \right)^2 + \frac{\eta_2}{\hbar^4} \chi_{01} \chi_{02} \mu_{1+}^2 \mu_{2-}^2,$$

$$\beta_6 = \frac{\eta_1}{\hbar^4} \chi_{01} \chi_{02} \mu_{1-}^2 \mu_{2+}^2 + \eta_2 \left(1 - \frac{\chi_{01}}{\hbar^2} \mu_{1+} \mu_{1-} \right)^2,$$

$$\beta_7 = \eta_1 \frac{\chi_{02}}{\hbar^2} \mu_{2+}^2 + \eta_2 \frac{\chi_{01}}{\hbar^2} \mu_{1+}^2,$$

$$\beta_8 = \eta_1 \frac{\chi_{01}}{\hbar^2} \mu_{1-}^2 \left(1 - \frac{\chi_{02}}{\hbar^2} \mu_{2+} \mu_{2-} \right)^2 + \eta_2 \frac{\chi_{02}}{\hbar^2} \mu_{2-}^2 \left(1 - \frac{\chi_{01}}{\hbar^2} \mu_{1+} \mu_{1-} \right)^2. \quad (35)$$

The coefficients η_1 and η_2 , in Eq. (35), are defined as

$$\eta_1 = -\lambda \kappa_{1+} \kappa_{2-} e^{(i/\hbar)2(\chi_{02} \mu_{02} - \chi_{01} \mu_{01})},$$

$$\eta_2 = -\lambda \kappa_{1-} \kappa_{2+} e^{(i/\hbar)2(\chi_{01} \mu_{01} - \chi_{02} \mu_{02})}. \quad (36)$$

The algebraic structure is not close in Hamiltonian (34); the time-evolution operator $\mathcal{U}_I^{(1)}(t)$ could not be written as the product of exponential operators. It can be obtained by using the Magnus approximation

$$\mathcal{U}_I^{(1)}(t) = \exp \left[\sum_{m=1}^{\infty} \Gamma_m(t) \right], \quad (37)$$

where $\Gamma_m(t)$ denotes the integrals of m -fold multiple commutators. The first two terms of the Magnus propagators, for example, are [39,40]

$$\Gamma_1(t) = -\frac{i}{\hbar} \int_0^t dt_1 \mathcal{H}_I^{(1)'}(t_1),$$

$$\Gamma_2(t) = \frac{1}{2\hbar^2} \int_0^t dt_2 \int_0^{t_2} dt_1 [\mathcal{H}_I^{(1)'}(t_1), \mathcal{H}_I^{(1)'}(t_2)]. \quad (38)$$

The total time-evolution operator $\mathcal{U}_I(t)$ of the whole system can be calculated by using Eq. (31). The transition probability from state $|v_{1i}, v_{2i}\rangle$ to state $|v_{1f}, v_{2f}\rangle$ is

$$P_{if}(t) = |\langle v_{1f}, v_{2f} | \mathcal{U}_I(t) | v_{1i}, v_{2i} \rangle|^2. \quad (39)$$

The explicit expression of the vibrational transition probability can be obtained and is given in the Appendix. The average energy in bonds can also be obtained by using the time-evolution operator.

III. NUMERICAL RESULTS AND DISCUSSIONS

A. Diatomic molecules

In this section, we study the multiphoton transition of the diatomic molecules. For comparison with the previous study, we use the local OH and OD bond of the HOD molecule in our numerical model. These models are extensively studied in a previous study [41–44]. All parameters, in atomic units, are taken from Refs. [41–44], namely, $\omega_0 = 0.01664$ a.u., $\chi_0 = 0.02323$ a.u., $D = 0.1614$ a.u., and $\alpha = 1.156$ a.u. for OH and

TABLE I. Multiphoton vibrational transition of OH. (All parameters are atomic units except n .)

	P_1	P_2	P_3	P_4	P_5	P_6
ω_r	0.016 253	0.015 480	0.014 707	0.013 934	0.013 161	0.012 388
n	1	2	3	4	5	6
ω_n	0.016 221	0.015 835	0.015 453	0.015 063	0.014 698	0.014 359
$ \omega_n - \omega_r $	0.000 032	0.000 355	0.000 746	0.001 129	0.001 537	0.001 971

TABLE II. Multiphoton vibrational transition of OD. (All parameters are atomic units except n .)

	P_1	P_2	P_3	P_4	P_5	P_6
ω_r	0.011 999	0.011 598	0.011 197	0.010 796	0.010 395	0.009 994
n	1	2	3	4	5	6
ω_n	0.011 963	0.011 716	0.011 556	0.011 474	0.011 192	0.010 959
$ \omega_n - \omega_r $	0.000 036	0.000 118	0.000 359	0.000 678	0.000 797	0.000 965

$\omega_0=0.0122$ a.u., $\chi_0=0.01645$ a.u., $D=0.1636$ a.u., and $\alpha = 1.142$ a.u. for OD, respectively.

1. Multiphoton vibrational transition

We first consider the following simple case: *The multiphoton vibrational transition*. In this case, we choose the laser field as follows:

$$\mathcal{E}(t) = \mathcal{E}_0 \sin(\omega_L t). \quad (40)$$

The initial state of the molecules are set on the ground state. The frequency of the infrared laser field is adjusted to the resonant frequency ω_r .

Multiphoton transitions are said to be in resonance if the energy of one or several quanta of laser is close to the transition energy from the initial to an intermediate excited state or to that between the intermediate. The transition is called multiphoton resonance transition, if the following condition is satisfied [45]:

$$\omega_r \cong \omega_n = \frac{(\varepsilon_f - \varepsilon_0)}{n\hbar}, \quad (41)$$

where $\varepsilon_f - \varepsilon_0$ is the energy gap between the ground state and the f th excited state.

Figures 1 and 2 give the long-time average probabilities of OH and OD from the ground state to the different excited states using Eq. (7). We can obtain the resonance frequency ω_r corresponding to the peaks of the transition probabilities. The orders of multiphoton transitions could be determined using *the formal intensity law* [46],

$$\ln P_n = n \ln I + C, \quad (42)$$

where I is the intensity of the laser field, P_n is the transition probability for the n -photon process, and C is a constant.

If no saturation occurs, one can determine the order of the multiphoton transition from the slope of Eq. (42). In Figs. 3 and 4 we give the log-log plots of the transition probabilities as a function of laser intensity I from the ground state to the different excited states. The order of the n -photon transition could be known from the slopes of Figs. 3 and 4, which correspond to the transition probabilities in Figs. 1 and 2, respectively. We have noted them in the figures, and detailed results are summarized in Table I and Table II.

As shown in Table I and Table II, the transitions from the ground state to the first, second, third, fourth, fifth, and sixth excited states belong to one-, two-, three-, four-, five-, and six-photon transitions. However, the deviation between the

transition frequency ω_r and the frequency ω_n is becoming larger. This deviation denotes that the nonresonant transition appears when the vibrational state goes up.

From Figs. 1 and 2, we can also see that the resonance frequencies ω_r are shifting a little when the system reaches the different final states. Namely, the resonant transition frequency decreases with the final energy level going up. And because of the higher dissociation energy in the deuterated case the transition probabilities of OD are all smaller than those of OH at the same laser intensity. The value of the interval between the transition peaks in Fig. 1 is about 0.000 773 a.u., and the value in Fig. 2 is about 0.000 401 a.u. The interval of the transition peaks of OH is larger than that of OD. We attribute it to the difference of the anharmonicity parameter of OH and OD, i.e., the anharmonic parameters of OH is larger than that of OD. The ratio of the anharmonicity parameters of OH and OD is 1.4 which is comparable to the ratio of 0.000773 to 0.000401 (≈ 1.9). Furthermore, we can see the deviations ($\omega_r - \omega_n$) of OH are also larger than those of OD in Table I and Table II. These results show the anharmonicity of molecular vibrations has an important influence on the resonant transition frequency.

2. Multiphoton selective vibrational transition of OH

Sugimori *et al.* investigated the multiphoton absorption of OH using numerical simulation [47]. For comparison, we take here the same molecular parameters as in Ref. [47]. We compare all the calculations for the one-photon, two-photon, three-photon, and four-photon absorption in Ref. [47] with our analytical results. In this comparison, the laser field is employed with the same as Ref. [47], namely,

$$\mathcal{E}(t) = \mathcal{E}_{0g}(t)\sin(\omega_L t),$$

TABLE III. Comparison of maximum laser intensity I_{\max} (W/cm²) and the ratio of the target state population between our algebraic model and other numerical results.

	OH ^a		OH	
	I_{\max}	Ratio (%)	I_{\max}	Ratio (%)
One-photon	4.74×10^6	100.00	4.68×10^6	99.99
Two-photon	5.68×10^8	99.98	5.57×10^8	99.49
Three-photon	5.58×10^9	99.88	5.42×10^9	99.23
Four-photon	2.36×10^{10}	94.51	2.27×10^{10}	95.31
Five-photon			8.21×10^{10}	95.07
Six-photon			1.79×10^{11}	94.92

^aNumerical solution from Ref. [47].

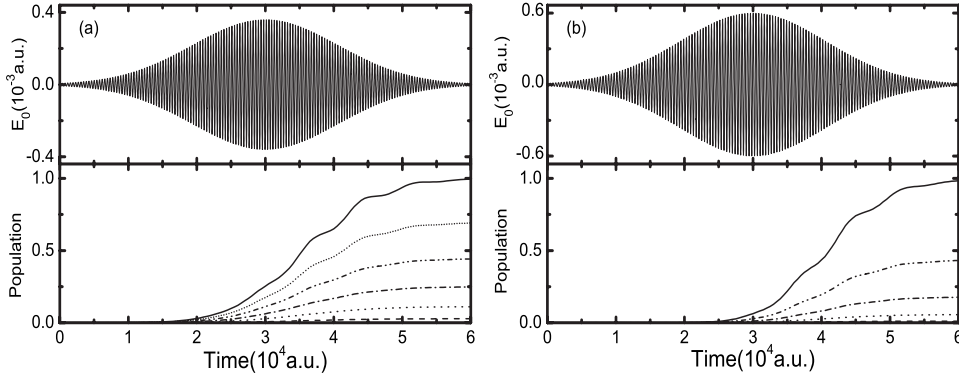


FIG. 5. Time dependence of the laser field and population: (a) One-photon transition between $|0\rangle$ and $|1\rangle$; (b) two-photon transition between $|0\rangle$ and $|2\rangle$, by changing the laser intensity with the fixed pulse duration at the nonchirped laser pulse. The laser parameters are given in Sec. III A 3.

$$g(t) = \exp[-(t - T_0)^2/\sigma^2], \quad (43)$$

where $T_0=100$ ps, $\sigma=30$ ps, and the laser frequency ω_L is calculated using Eq. (41). In Table III a comparison is made between numerical results in Ref. [47] and our analytical results. A good agreement is found. The results of five- and six-photon are also given by our algebraic model, and they are also listed in the table. Since there exists a little deviation of the resonant transition frequency for the different transition (see details in Table I and Table II), we then take the calculated frequency as the laser frequency and study the multiphoton selective vibrational transition of OH. We find the selectivity of the vibrational transition will decrease as the value of the laser frequency has a little change (about 0.000001 a.u. $\approx 6.6 \times 10^3$ MHz). The little changes on the laser frequency may cause less selectivity and stronger laser intensity. This denotes the selectivity of vibrational transition is sensitive to the laser frequency.

3. Control of vibrational excitation of OH and OD molecules

We have obtained the resonant transition frequencies of OH and OD from the ground state to some excited states in the previous section. In this section, we use these resonant frequencies to study the selective vibrational transition of OH and OD. The laser field is

$$\mathcal{E}(t) = \mathcal{E}_0 f(t) \cos \Phi(t),$$

$$f(t) = \exp[-(t - \pi/2)^2/(\pi/4)^2], \quad (44)$$

where the Gaussian pulse envelope $f(t)$ is employed since it is extensively employed in experiment [5]. The frequency of the field is chosen constant for nonchirped laser pulses (ω_r) or time dependent for chirped ones, namely, the phase of the laser field pulse is chosen as

$$\Phi(t) = \begin{cases} \omega_r t & (\text{nonchirped pulse}), \\ \Phi_0 + \int_0^t [\Delta \omega_1 + \Delta \omega_2 e^{-t'/\tau}] dt' & (\text{chirped pulse}). \end{cases} \quad (45)$$

That is, the two types of the laser pulse are used to study the selective vibrational transition: *The nonchirped laser pulse and the chirped laser pulse.*

The selective excitations of one-photon and two-photon of OH are first studied by the nonchirped laser pulse. The pulsewidth is set to be $\tau=60000$ a.u. (≈ 1.4 ps) as in Refs. [48,49]. We adjust the laser intensity to get maximum populations from $\mathcal{E}_0=0.000055$ a.u. to $\mathcal{E}_0=0.00033$ a.u. ($\approx 0.4 \times 10^{10}$ W/cm²) for one-photon, and from $\mathcal{E}_0=0.00013$ a.u.

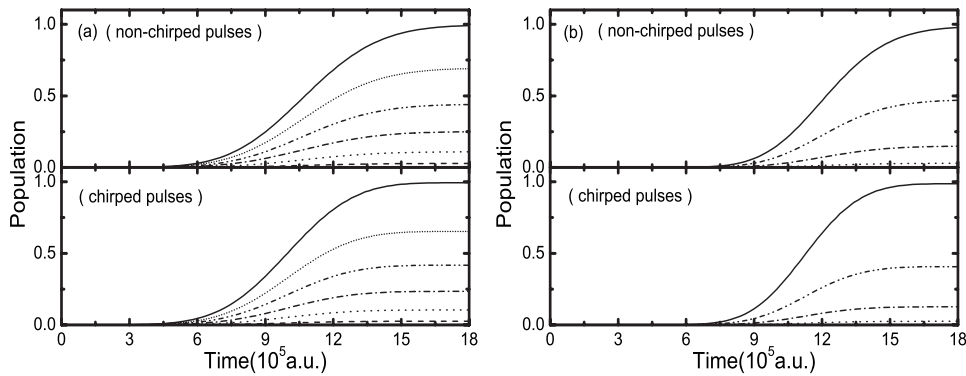


FIG. 6. Comparison of populations between the chirped by changing the laser intensity with the fixed pulse duration. (a) One-photon transition between $|0\rangle$ and $|1\rangle$; the value of the laser field strength from the lowest curve to the highest one in the nonchirped pulse is from $\mathcal{E}_0=0.000001$ a.u. to $\mathcal{E}_0=0.000011$ a.u. ($\approx 4.25 \times 10^6$ W/cm²), and in the chirped pulse is from $\mathcal{E}_0=0.0000017$ a.u. to $\mathcal{E}_0=0.0000102$ a.u. ($\approx 3.59 \times 10^6$ W/cm²). (b) Two-photon transition between $|0\rangle$ and $|2\rangle$; the value of the laser field strength from the lowest curve to the highest one in the nonchirped pulse is from $\mathcal{E}_0=0.00004$ a.u. to $\mathcal{E}_0=0.00012$ a.u. ($\approx 5.05 \times 10^8$ W/cm²), and in the chirped pulse is from $\mathcal{E}_0=0.00003$ a.u. to $\mathcal{E}_0=0.00011$ a.u. ($\approx 4.29 \times 10^8$ W/cm²).

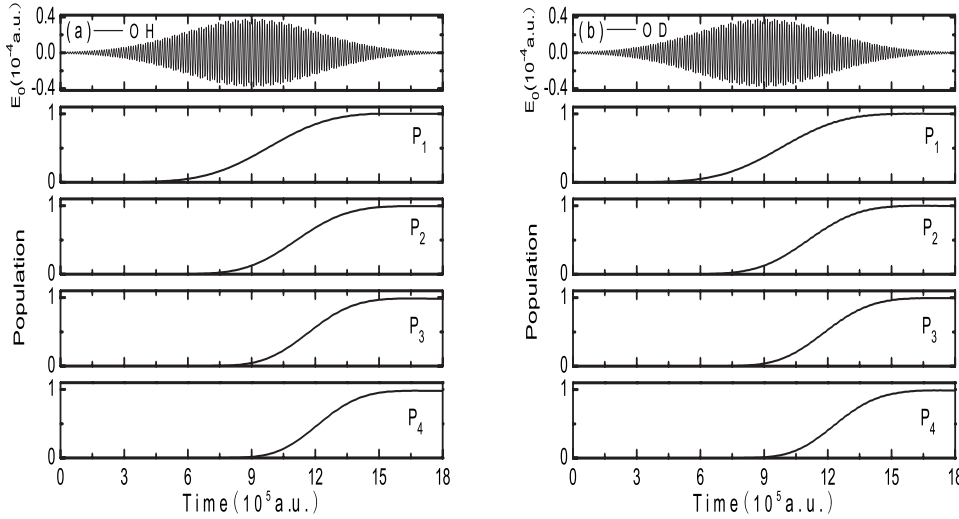


FIG. 7. Time dependence of the laser field and the maximum population P_1, P_2, P_3, P_4 : (a) For OH; (b) for OD. The optimal parameters are listed in Table IV.

to $\mathcal{E}_0=0.00065$ a.u. ($\approx 0.15 \times 10^{11}$ W/cm²) for two-photon. In Fig. 5 we plot the time dependence of the laser field and population with different intensity. From Fig. 5 we see that the oscillations appearing in the population with the laser intensity increases under the condition of the laser pulse duration are relatively small. To avoid the oscillations, we adjust the laser pulse duration. We find that the oscillations disappear completely at the pulsewidth $\tau=18 \times 10^5$ a.u. (≈ 40 ps). This value is consistent with the pulsewidth in Ref. [47]. Then we study the changes of the transition probabilities when the nonchirped laser pulse is turned to the chirped one. The transitions from the ground state to the first and second excited states at different laser intensity are given in Fig. 6. The laser intensity begins to increase from a relative small value till the populations get the maximum values at the end of the nonchirped or chirped pulse (see Fig. 6 caption). For the chirped pulse, we take the frequency $\Delta\omega_1$ as the resonant frequency, namely, we let $\Delta\omega_1=\omega_r$. The chirped term $\Delta\omega_2$ is adjusted to get a good selectivity at a certain laser intensity. From Fig. 6, we can see that the populations begin to increase and get the maximum earlier by the chirped pulse than the nonchirped one. It shows the chirped pulse gives better control of vibrational excitation of molecules. Finally, we give the selective excitation of one-photon, two-photon, three-photon, and four-photon of OH and OD. Figure 7 gives the maximum populations of the target states; the populations of other transitions are all

smaller than 10^{-6} and decrease rapidly. We can obtain complete selective vibrational excitation by a Gaussian shaped and chirped laser pulse. The optimal parameters of the laser pulse are given in Table IV. We find the values of the chirped term of OH are larger than those of OD which could also be relevant to the anharmonicity of molecular vibrations. In the same laser duration, the laser frequency of OH decreases faster than that of OD, but the laser intensity of OD is higher than that of OH.

From the above discussion, we see that the optimal laser frequency must decrease as a function of time in order to achieve a good selectivity of excitation. Furthermore, the chirping of OH is faster than that of OD.

B. Triatomic molecules

In this section we study the control of triatomic molecules. As for triatomic molecules, there exists richer information of selective laser excitation, for example, there is the phenomenon of intramolecular vibrational redistribution (IVR). The IVR can interfere with selective excitation. Here we investigate the direct resonant excitation of the intramolecular bond for linear triatomic molecules HCN and DCN.

The Hamiltonian (20) is used to calculate the stretch vibrational levels of HCN and DCN molecules successfully, and it can reproduce the real situations of the molecules [36]. The molecular parameters of HCN and DCN, in our current

TABLE IV. The optimal laser parameters of multiphoton selective vibrational excitation of OH and OD.

	OH			OD		
	$\Delta\omega_1$ (a.u.)	$\Delta\omega_2$ (a.u.)	I_{\max} (W/cm ²)	$\Delta\omega_1$ (a.u.)	$\Delta\omega_2$ (a.u.)	I_{\max} (W/cm ²)
One-photon	0.016 253	0.000 004 2	3.59×10^6	0.011 999	0.000 004 0	4.80×10^6
Two-photon	0.015 480	0.000 004 0	4.29×10^8	0.011 598	0.000 003 3	5.61×10^8
Three-photon	0.014 707	0.000 003 8	4.25×10^9	0.011 197	0.000 002 5	5.05×10^9
Four-photon	0.013 934	0.000 003 6	1.76×10^{10}	0.010 796	0.000 001 8	1.91×10^{10}
Five-photon	0.013 161	0.000 003 4	7.68×10^{10}	0.010 395	0.000 001 2	8.04×10^{10}
Six-photon	0.012 388	0.000 003 2	1.03×10^{11}	0.009 994	0.000 000 6	1.32×10^{11}

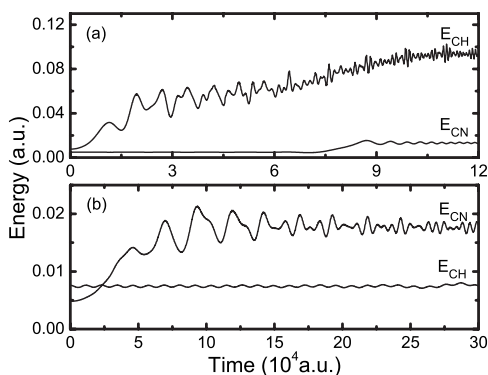


FIG. 8. Selective excitation of C-H bond and C-N bond for HCN to the $v=10$ level by a resonance linearly chirped pulse with a rectangular shape. (a) Time dependence of energy in C-H bond (E_{CH}) and in C-N bond (E_{CN}). The pulse parameters are $I=0.9 \times 10^{12}$ W/cm 2 ; $\alpha_c=0.38$; $\tau \approx 2.8$ ps. (b) Time dependence of energy in C-H bond (E_{CH}) and in C-N bond (E_{CN}). The pulse parameters are $I=0.5 \times 10^{13}$ W/cm 2 ; $\alpha_c=0.13$; $\tau \approx 7.2$ ps.

numerical calculations, are taken from Ref. [36].

We investigate the effects of linearly chirped pulses with different shapes on the molecules. The linearly chirped pulses are successfully used to study vibrational excitation and dissociation of the molecules [50–52]. Furthermore, a linearly chirped pulse can be readily prepared in the laboratory [53,54]. The laser field is as follows:

$$\mathcal{E}(t) = \mathcal{E}_0 f(t) \cos \Phi(t),$$

$$\Phi(t) = \Omega_0 t \left(1 - \frac{\alpha_c t}{2\tau} \right). \quad (46)$$

In our numerical calculation, Ω_0 is taken as the anharmonic frequency of the selected bond, namely, we let $\Omega_0 = \omega_{01}$ or ω_{02} . The instantaneous frequency is taken as $\Omega_{\text{ins}}(t) = \Omega_0 [1 - \alpha_c(t/\tau)]$; the amount of chirping is then determined by the parameters α_c . The target excitation state is chosen $v=10$

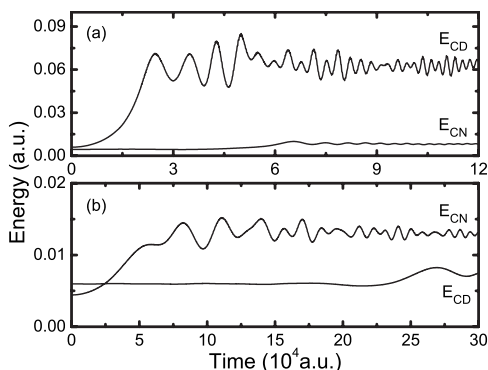


FIG. 9. Selective excitation of C-D bond and C-N bond for DCN to the $v=10$ level by a resonance linearly chirped pulse with a rectangular shape. (a) Time dependence of energy in C-D bond (E_{CD}) and in C-N bond (E_{CN}). The pulse parameters are same as in Fig. 8(a) except $\alpha_c=0.26$. (b) Time dependence of energy in C-D bond (E_{CD}) and in C-N bond (E_{CN}). The pulse parameters are same as in Fig. 8(b) except $\alpha_c=0.11$.

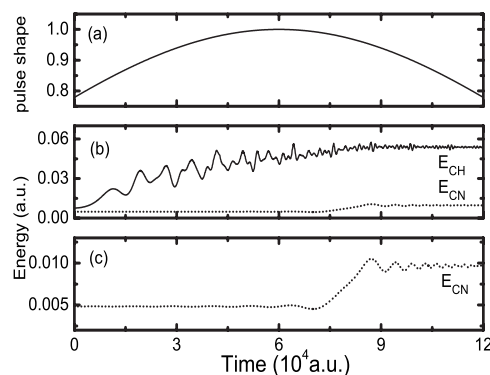


FIG. 10. Selective excitation of C-H bond of HCN to the $v=10$ level by a resonance linearly chirped pulse with a Gaussian shape. (a) Time dependence of Gaussian pulse shape: $f(t) = \exp[-(t-\tau/2)^2/\tau^2]$. (b) Time dependence of energy in C-H bond (solid lines for E_{CH}) and in C-N bond (dotted lines for E_{CN}). (c) The enlargement of C-H bond energy in panel (b). The pulse parameters are the same as in Fig. 8(a).

which determines the value of the parameters α_c . Research as in Refs. [55,56] shows the ionization threshold is estimated to be at 10^{14} W/cm 2 , the laser intensities chosen in this investigation are all far below this value, and other parameters are similar to Ref. [57] and given in figure captions. We consider here three kinds of laser shapes: *Rectangular*, *Gaussian* and *sech-shaped*.

1. Selective bond excitation via the rectangular laser shape

The selective vibrational excitation of C-H (C-D) and C-N bonds can be achieved by using the *rectangular laser shape* as shown in Figs. 8 and 9. The selective target bond picks up a higher energy but the energy of the other bond has a relatively smaller value at the end of the pulse. The selective bond excitation in molecule HCN is plotted in Fig. 8. In Fig. 8(a), we can see the energy in the C-N bond does not oscillate around the initial energy but it has a pronounced increase after the energy in the C-H bond grows. There are two possibilities about this phenomenon. One is due to the intramolecular vibrational redistribution (IVR) as energy leaks from the highly excited C-H bond; the other is due to

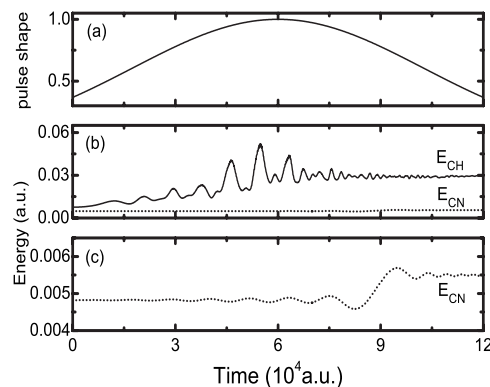


FIG. 11. Same as Fig. 10, except $f(t) = \exp[-(t-\tau/2)^2/(\tau/2)^2]$.

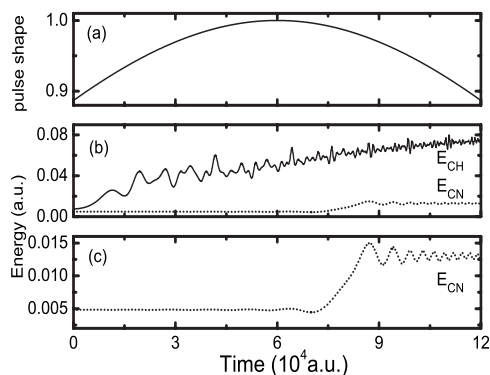


FIG. 12. Selective excitation of C-H bond of HCN to the $v=10$ level by a sech-shaped and resonance linearly chirped pulse. (a) Time dependence of sech-shaped pulse shape: $f(t)=\text{sech}[(t-\tau/2)/\tau]$. (b) Time dependence of energy in C-H bond (solid lines for E_{CH}) and in C-N bond (dotted lines for E_{CN}). (c) The enlargement of C-N bond energy in panel (b). The pulse parameters are the same as in Fig. 8(a).

an accidental resonance with the pulse frequency which is near the C-N frequency (ω_{02}) at the end of the laser pulse. From Fig. 8(b), we see the selective vibrational excitation of the C-N bond needs longer pulse duration and higher laser intensity. The C-N bond is much heavier and stronger than the C-H bond, so the C-H bond may break first before the C-N bond is excited to the higher excitation level or dissociation and the selectivity of the C-N bond decreases. The results are consistent with the other study [57].

The selective vibrational excitation of DCN is given in Fig. 9 and a similar case is observed. However, from Fig. 9(a), we can see that the energy in the C-D bond does not always increase but begins to oscillate after some time, and the energy in the C-N bond begins to increase earlier than that of HCN. In Fig. 9(b) when the C-N bond is excited, the C-D bond picks up energy at the end of the pulse. Compared to Fig. 8, energies in the selective C-D bond or the selective C-N bond are smaller than those of HCN. These results rep-

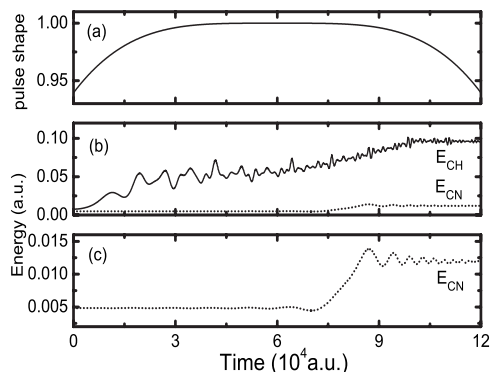


FIG. 13. Selective excitation of C-H bond of HCN to the $v=10$ level by a resonance linearly chirped pulse with a super-Gaussian shape. (a) Time dependence of super-Gaussian pulse shape: $f(t)=\exp[-(t-\tau/2)^4/\tau^4]$. (b) Time dependence of energy in C-H bond (solid lines for E_{CH}) and in C-N bond (dotted lines for E_{CN}). (c) The enlargement of C-N bond energy in panel (b). The pulse parameters are the same as in Fig. 8(a).

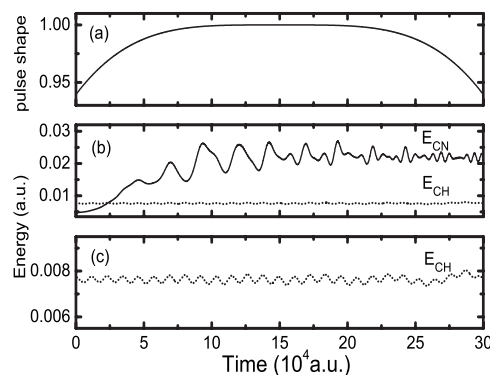


FIG. 14. Selective excitation of C-N bond of HCN to the $v=10$ level by a resonance linearly chirped pulse with a super-Gaussian shape. (a) Time dependence of super-Gaussian pulse shape: $f(t)=\exp[-(t-\tau/2)^4/\tau^4]$. (b) Time dependence of energy in C-N bond (solid lines for E_{CN}) and in C-H bond (dotted lines for E_{CH}). (c) The enlargement of C-N bond energy in panel (b). The pulse parameters are the same as in Fig. 8(b).

resent the fact that IVR (intramolecular vibrational redistribution) in the DCN molecule is faster and the selectivity of DCN is much less than that of HCN which is consistent with Ref. [58].

2. C-H bond excitation in HCN molecule by a Gaussian and sech-shaped laser pulses

Figures 10 and 11 show that the oscillations of energy in the C-H bond decreased at the end of the Gaussian shaped laser pulse and the pulsewidth of the Gaussian shape has a deep influence on oscillations of energy. But the energy in the C-H bond also decreases in the Gaussian shaped laser pulse and the value is smaller than in the rectangular laser pulse. In contrast, using the sech-shaped laser pulses, the value of energy becomes large but still smaller than in the rectangular laser pulse as shown in Fig. 12.

From these two figures, we find the values of energy in the bond excitation is decided by the pulse area, and the oscillations of energy are related to the pulse shape. In order to get small oscillation and high energy, we take a super-Gaussian shape laser pulse and give the C-H and C-N bond selective excitation in Fig. 13 and Fig. 14. As we expected, the energy in the C-H bond has larger values and smaller oscillations compared to the other shaped cases. The C-N bond excitation also has a better selectivity than the rectangular case at the same laser intensity.

IV. CONCLUSION

We have studied selective vibrational excitation for small molecules in an algebraic model. State-selective excitation of diatomic molecules and bond selective excitation of triatomic molecules is achieved successfully. The results are in good agreement with other research. In this investigation, we find the optimal laser frequency must decrease as a function of time and the transition probability is very sensitive to the laser frequency to the control state excitation of a diatomic molecule. For the triatomic molecule, although the intramo-

lecular vibrational redistribution makes selective excitation difficult, selective excitation to a specific vibrational bond can be achieved by using the appropriate chirped and shaped pulse. To get a good selectivity of bond excitation, the pulse area and the pulse shape are of the same importance. The pulse area decides the value of energy in bonds and the proper laser shape decreases the oscillations of energy. In our cases, a super-Gaussian shape laser can be used to obtain a better selectivity of bond excitation. Furthermore, the bending motions and rotations can be taken into account and this method can also be extended to study the tetra-atomic molecular case.

ACKNOWLEDGMENTS

This work was supported by the National Science Foundation of China (Grant Nos. 10674083 and 10474058) with partial financial support from the Science Foundation of Shandong Province, China.

APPENDIX

The transition probability of the triatomic molecule is introduced in this appendix. From Eqs. (31) and (39) we have

$$P_{if}(t) = |\langle v_{1f}, v_{2f} | \mathcal{U}_I^{(0)}(t) \mathcal{U}_I^{(1)}(t) | v_{1i}, v_{2i} \rangle|^2. \quad (\text{A1})$$

We split the transition probability into two parts for simplicity: One is the term obtained by using the time evolution operator $\mathcal{U}_I^{(0)}(t)$ [see Eq. (29)]; the other is obtained by the Magnus approximation. During the computation, we found that the values of $\beta_k(t)$ ($k=0, 1, 2, \dots, 8$) are much smaller than $\mu_r(t)$ ($r=0, \pm$); we take one term, in the Magnus approximation, i.e.,

$$\mathcal{U}_I^{(1)}(t) \approx e^{\Gamma_1(t)}. \quad (\text{A2})$$

In the calculation of the explicit expression of \mathcal{P}_{if} in Eq. (A1) we used

$$\begin{aligned} \Gamma_1(t) |v_{1i}, v_{2i}\rangle = & \alpha_0(t)(1 - 2\chi_{01}v_{1i})(1 - 2\chi_{02}v_{2i}) |v_{1i}, 0, v_{2i}\rangle + \alpha_1(t)(1 - 2\chi_{02}v_{2i}) \sqrt{(1 - \chi_{01}v_{1i})(v_{1i} + 1)} |v_{1i} + 1, v_{2i}\rangle \\ & + \alpha_2(t)(1 - 2\chi_{02}v_{2i}) \sqrt{[1 - \chi_{01}(v_{1i} - 1)]} |v_{1i} - 1, v_{2i}\rangle \\ & + \alpha_3(t)(1 - 2\chi_{01}v_{1i}) \sqrt{(1 - \chi_{02}v_{2i})(v_{2i} + 1)} |v_{1i}, v_{2i} + 1\rangle \\ & + \alpha_4(t)(1 - 2\chi_{01}v_{1i}) \sqrt{[1 - \chi_{02}(v_{2i} - 1)]} |v_{1i}, v_{2i} - 1\rangle \\ & + \alpha_5(t) \sqrt{(1 - \chi_{01}v_{1i})(v_{1i} + 1)} \sqrt{[1 - \chi_{02}(v_{2i} - 1)]} |v_{1i} + 1, v_{2i} - 1\rangle \\ & + \alpha_6(t) \sqrt{[1 - \chi_{01}(v_{1i} - 1)]} |v_{1i} - 1, v_{2i} + 1\rangle \\ & + \alpha_7(t) \sqrt{(1 - \chi_{01}v_{1i})(v_{1i} + 1)} \sqrt{(1 - \chi_{02}v_{2i})(v_{2i} + 1)} |v_{1i} + 1, v_{2i} + 1\rangle \\ & + \alpha_8(t) \sqrt{[1 - \chi_{01}(v_{1i} - 1)]} |v_{1i} - 1, v_{2i} - 1\rangle, \end{aligned} \quad (\text{A3})$$

where $\alpha_k(t) = \int_0^t \beta_k(t') dt'$ ($k=0, 1, 2, \dots, 8$), by using the first Magnus approximation $\mathcal{U}_I^{(1)}(t) = \exp[-\int_0^t \mathcal{H}_I^{(1)}(t') dt']$.

The time evolution operator $\mathcal{U}_I^{(0)}(t)$ acting on the vibrational state $|v_1, v_2\rangle$ is given by

$$\begin{aligned} \mathcal{U}_I^{(0)}(t) |v_1, v_2\rangle = & \exp\left\{-\frac{i}{\hbar} \mu_{02} [1 - 2\chi_{02}(v_2 - m_2 + n_2)]\right\} \sum_{n_2=0}^{\infty} \frac{1}{n_2!} \left(-\frac{i}{\hbar} \mu_{2+}\right)^{n_2} \sqrt{\prod_{n'_2=0}^{n_2} [1 - \chi_{02}(v_2 - m'_2 + n'_2)]} (v_2 - m'_2 + n'_2) \\ & \times \sum_{m_2=0}^{\infty} \frac{1}{m_2!} \left(-\frac{i}{\hbar} \mu_{2-}\right)^{m_2} \sqrt{\prod_{m'_2=0}^{m_2} [1 - \chi_{02}(v_2 - m'_2)(v_2 - m'_2 + 1)]} \exp\left\{-\frac{i}{\hbar} \mu_{01} [1 - 2\chi_{01}(v_1 - m_1 + n_1)]\right\} \\ & \times \sum_{n_1=0}^{\infty} \frac{1}{n_1!} \left(-\frac{i}{\hbar} \mu_{1+}\right)^{n_1} \sqrt{\prod_{n'_1=0}^{n_1} [1 - \chi_{01}(v_1 - m'_1 + n'_1)]} (v_1 - m'_1 + n'_1) \\ & \times \sum_{m_1=0}^{\infty} \frac{1}{m_1!} \left(-\frac{i}{\hbar} \mu_{1-}\right)^{m_1} \sqrt{\prod_{m'_1=0}^{m_1} [1 - \chi_{01}(v_1 - m'_1)(v_1 - m'_1 + 1)]}. \end{aligned} \quad (\text{A4})$$

Combing Eq. (A3) with Eq. (A4), putting them into Eq. (A1), and after some algebra, the explicit expression of the vibrational transition probability $\mathcal{P}_{if}(t)$ is obtained.

- [1] D. J. Tannor and S. A. Rice, *J. Chem. Phys.* **83**, 5013 (1985).
- [2] P. Brumer and M. Shapiro, *Chem. Phys. Lett.* **126**, 54 (1986).
- [3] R. S. Judson and H. Rabitz, *Phys. Rev. Lett.* **68**, 1500 (1992).
- [4] R. J. Levis, G. M. Menkir, and H. Rabitz, *Science* **292**, 709 (2001).
- [5] S. Zou, Q. Ren, G. G. Balint-Kurti, and F. R. Manby, *Phys. Rev. Lett.* **96**, 243003 (2006).
- [6] R. J. Gordon and S. A. Rice, *Annu. Rev. Phys. Chem.* **48**, 601 (1997).
- [7] S. A. Rice and M. Zhao, *Optical Control of Molecular Dynamics* (Wiley, New York, 2000).
- [8] P. Brumer and M. Shapiro, *Coherent Control of Atomic and Molecular Process* (Wiley, New York, 2003).
- [9] P. Kral, I. Thanopoulos, and M. Shapiro, *Rev. Mod. Phys.* **79**, 53 (2007).
- [10] S. C. Leasure, K. F. Milfeld, and R. E. Wyatt, *J. Chem. Phys.* **74**, 6197 (1981).
- [11] P. G. Burke, J. Colgan, D. H. Glass, and K. Higgins, *J. Phys. B* **33**, 143 (2000).
- [12] J. Colgan, D. H. Glass, K. Higgins, and P. G. Burke, *J. Phys. B* **34**, 2089 (2001).
- [13] S. Chu and D. A. Telnov, *Phys. Rep.* **390**, 1 (2004).
- [14] F. Iachello, *Chem. Phys. Lett.* **78**, 581 (1981).
- [15] O. S. van Roosmalen, I. Benjamin, and R. D. Levine, *J. Chem. Phys.* **81**, 5986 (1984).
- [16] I. Benjamin, R. D. Levine, and J. L. Kinsey, *J. Phys. Chem.* **87**, 727 (1983).
- [17] S. Ding and Y. Zheng, *J. Chem. Phys.* **111**, 4466 (1999).
- [18] Y. Zheng and S. Ding, *Phys. Rev. A* **64**, 032720 (2001).
- [19] Y. Zheng and S. Ding, *Phys. Lett. A* **256**, 197 (1999).
- [20] C. D. Batista and G. Ortiz, *Adv. Phys.* **53**, 1 (2004).
- [21] K. Kikoin, Y. Avishai, and M. N. Kiselev, e-print arXiv:cond-mat/0407063.
- [22] I. P. Vadeiko, G. P. Miroshnichenko, A. V. Rybin, and J. Timonen, *Phys. Rev. A* **67**, 053808 (2003).
- [23] A. R. P. Rau and W. Zhao, *Phys. Rev. A* **71**, 063822 (2005).
- [24] Y. Zheng, *Phys. Rev. A* **74**, 066101 (2006).
- [25] X. W. Hou, J. H. Chen, and Z. Q. Ma, *Phys. Rev. A* **74**, 062513 (2006).
- [26] R. D. Levine, *Chem. Phys. Lett.* **95**, 87 (1983).
- [27] M. E. Kellman, *J. Chem. Phys.* **82**, 3300 (1985).
- [28] I. L. Cooper and R. K. Gupta, *Phys. Rev. A* **55**, 4112 (1995).
- [29] I. L. Cooper, *J. Phys. Chem. A* **102**, 9565 (1998).
- [30] P. J. Hay and T. H. Dunning, *J. Chem. Phys.* **64**, 5077 (1976).
- [31] R. B. Walker and R. K. Preston, *J. Chem. Phys.* **67**, 2017 (1977).
- [32] M. Tung and J. M. Yuan, *Phys. Rev. A* **36**, 4463 (1987).
- [33] S. Chelkowski, A. D. Bandrauk, and P. B. Corkum, *Phys. Rev. Lett.* **65**, 2355 (1995).
- [34] Y. Alhassid and R. D. Levine, *Phys. Rev. A* **18**, 89 (1978).
- [35] J. Wei and E. Norman, *Proc. Am. Math. Soc.* **15**, 327 (1964).
- [36] H. Feng and S. Ding, *J. Phys. B* **40**, 69 (2007).
- [37] H. Umeda, M. Sugawara, Y. Fujimura, and S. Koseki, *Chem. Phys. Lett.* **229**, 233 (1994).
- [38] See, e.g., L. D. Landau and M. E. Lifshitz, *Quantum Mechanics* (Pergamon Press, New York, 1977).
- [39] S. Klarsfeld and J. A. Oteo, *Phys. Rev. A* **39**, 3270 (1989).
- [40] G. Dattoli, J. Gallardo, and A. Torre, *J. Math. Phys.* **27**, 772 (1986).
- [41] M. V. Korolkov and G. K. Paramonov, *Phys. Rev. A* **56**, 3860 (1997).
- [42] S. Stranges, R. Rithcer, and M. Alagia, *J. Chem. Phys.* **116**, 3676 (2002).
- [43] B. Amstrup and N. E. Henriksen, *J. Chem. Phys.* **97**, 8285 (1992).
- [44] N. Elghobashi, P. Krause, J. Manz, and M. Oppel, *Phys. Chem. Chem. Phys.* **5**, 4806 (2003).
- [45] W. Jakubetz, B. Just, J. Manz, and H. J. Schreier, *J. Phys. Chem.* **94**, 2294 (1990).
- [46] S. H. Lin and Y. Fujimura, *Multiphoton Spectroscopy of Molecules* (Academic Press, Inc., London, 1984).
- [47] K. Sugimori, T. Ito, H. Nagao, and K. Nishikawa, *Int. J. Quantum Chem.* **105**, 596 (2005).
- [48] B. Just, J. Manz, and I. Trisca, *Chem. Phys. Lett.* **193**, 423 (1992).
- [49] M. V. Korolkov, G. K. Paramonov, and B. Schmidt, *J. Chem. Phys.* **105**, 1862 (1996).
- [50] W. K. Liu, B. Wu, and J. M. Yuan, *Phys. Rev. Lett.* **75**, 1292 (1995).
- [51] W. K. Liu, J. M. Yuan, and S. H. Lin, *Phys. Rev. A* **60**, 1363 (1999).
- [52] J. T. Lin, T. L. Lai, D. S. Chuu, and T. F. Jiang, *J. Phys. B* **31**, L117 (1998).
- [53] T. Witte, T. Hornung, L. Windhorm, and D. Proch, *J. Chem. Phys.* **118**, 2021 (2003).
- [54] P. Balling, D. J. Maas, and L. D. Noordam, *Phys. Rev. A* **50**, 4276 (1994).
- [55] J. Gong, Ao Ma, and S. A. Rice, *J. Chem. Phys.* **122**, 144311 (2005).
- [56] C. M. Dion, A. Keller, O. Atabek, and A. D. Bandrauk, *Phys. Rev. A* **59**, 1382 (1999).
- [57] R. Brezina and W. Liu, *J. Phys. Chem. A* **108**, 8852 (2004).
- [58] S. Chelkowski and A. D. Bandrauk, *Chem. Phys. Lett.* **186**, 264 (1991).